*Acta Cryst.* (1995). D**51**, 1003–1012

# 1.6 Å Structure of a Semisynthetic Ribonuclease Crystallized from Aqueous Ethanol. Comparison with Crystals from Salt Solutions and with Ribonuclease A from Aqueous Alcohol Solutions

BY SRINI J. DE MEL, MARILYNN S. DOSCHER* AND PHILIP D. MARTIN

*Department of Biochemistry, Wayne State University School of Medicine, Detroit, MI*, 48201, *USA*

FRANCIS RODIER

*Laboratoire de Biologie Structurale, CNRS - Bâtiment* 34, *F* 91 198 *Gif sur Yvette, France*

AND BRIAN F. P. EDWARDS*

*Department of Biochemistry, Wayne State University School of Medicine, Detroit, MI*, 48201, *USA*

(*Received* 10 *February* 1995; *accepted* 30 *March* 1995)

## Abstract

The non-covalent combination of residues 1–118 of RNase A with a synthetic 14-residue peptide containing residues 111–124 of the molecule forms a highly active semisynthetic enzyme, RNase 1–118:111–124. With this enzyme, the roles played by the six C-terminal residues in generating the catalytic efficiency and substrate specificity of RNase can be studied using chemically synthesized analogs. The structure of RNase 1–118:111–124 from 43% aqueous ethanol has been determined using molecular-replacement methods and refined to a crystallographic *R* factor of 0.166 for all observed reflections in the range 7.0–1.6 Å (Protein Data Bank file 1SSC). The structure is compared with the 2.0 Å structure of RNase A from 43% aqueous 2-methyl-2-propanol and with the 1.8 Å structure of the semisynthetic enzyme obtained from crystals grown in concentrated salt solution. The structure of RNase 1–118:111–124 from aqueous ethanol is virtually identical to that of RNase A from aqueous 2-methyl-2-propanol. Half of the crystallographically bound water molecules are not coincident, however. The structure is somewhat less similar to that of RNase 1–118:111–124 from salt solutions, with a major difference being the positioning of active-site residue His119.

## Abbreviations

RNase A, bovine pancreatic ribonuclease A; RNase S, RNase A in which the 20–21 peptide bond has been hydrolyzed by the action of subtilisin; RNase 1–118, polypeptide consisting of residues 1–118 of RNase A; RNase 111–124, tetradecapeptide consisting of residues 111–124 of RNase A; RNase 1–118:111–124, noncovalent complex of RNase 1–118 and RNase 111–124, also referred to as the 'parent complex'; RNase 1–118:111–124[EtOH], RNase 1–118:111–124 crystallized from aqueous ethanol; RNase 1–118:111–124[salt], RNase 1–118:111–124 crystallized from concentrated salt solution; PDB, Brookhaven Protein Data Bank (Bernstein *et al.*, 1977).

## Introduction

Successive digestion by pepsin and by carboxypeptidase A of bovine pancreatic RNase A removes six residues from the C-terminus of the molecule to form a shortened chain, RNase 1–118, that is devoid of enzymatic activity (Lin, 1970).

Complementation of RNase 1–118 with a synthetic 14-residue peptide containing the C-terminus of the molecule, namely, residues 111–124, forms a semisynthetic noncovalent complex, RNase 1–118:111–124 ($K_D$ in the presence of substrate = 1 $\mu M$ at pH 6.0) that exhibits 98% of the enzymatic activity of RNase A (Fig. 1) (Lin, Gutte, Moore & Merrifield, 1970; Gutte, Lin, Caldi & Merrifield, 1972). The eight redundant

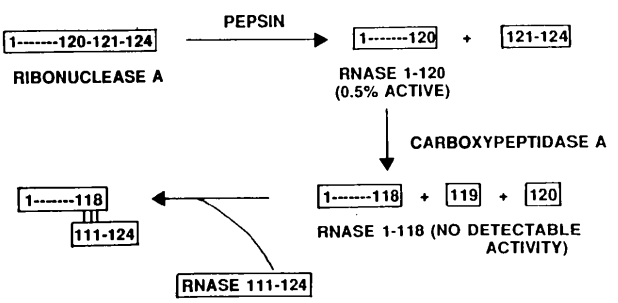


Fig. 1. Preparation and assembly of RNase 1–118:111–124. The schematic diagram shows the preparation of RNase 1–118 by proteolytic digestion and its assembly with a chemically synthesized 111–124 peptide into a non-covalent complex (which is fully active when no amino-acid replacements have been made).

* Authors for correspondence.

residues are needed to achieve good binding and full activity. The six C-terminal residues are unique to the peptide, however, allowing study through the chemical synthesis of structural variants of the peptide portion of the possible roles played by these residues in generating the catalytic efficiency and substrate specificity of the enzyme. Semisynthetic complexes between RNase 1–118 and a large number of structural analogs of RNase 111–124 have been prepared and characterized both kinetically (Lin, Gutte, Caldi, Moore & Merrifield 1972; Hodges & Merrifield, 1974; Hodges & Merrifield, 1975; Merrifield & Hodges, 1975; Serdijn, Hoes, Raap & Kerling, 1980; Stern & Doscher, 1984; Serdijn, Bloemhoff, Kerling & Havinga, 1984*a*) and by proton NMR measurements (Doscher, Martin & Edwards, 1983; Serdijn, Bloemhoff, Kerling & Havinga, 1984*b*; Cederholm, Stuckey, Doscher & Lee, 1991).

In addition, high-resolution crystal structures have been determined for several catalytically modified analogs (de Mel, Martin, Doscher & Edwards, 1992; de Mel *et al.*, 1994; de Mel, Doscher, Martin & Edwards, 1994) as well as for the fully active parent structure (Martin, Doscher & Edwards, 1987).

Up to this time, however, the most exact comparison of these structures with that of RNase A has not been possible as the crystals of the semisynthetic enzymes have been obtained from concentrated salt solutions, while those for RNase A have all been obtained from aqueous alcohol solutions. We report here a 1.6 Å structure of RNase 1–118:111–124 obtained with crystals grown from aqueous ethanol, henceforth referred to as RNase 1–118:111–124[EtOH], PDB file 1SSC (Bernstein *et al.*, 1977), under the same conditions used by Wlodawer and coworkers to grow the RNase A crystals used in their structural analyses of this protein (Wlodawer, Bott & Sjölin, 1982; Wlodawer & Sjölin, 1983; PDB file 5RSA). The determination of the structure of RNase 1–118:111–124 in crystals grown from an aqueous organic mother liquor also allows a comparison with the 1.8 Å structure of exactly the same protein obtained with crystals grown from concentrated salt solutions, henceforth referred to as RNase 1–118:111–124[salt] (Martin *et al.*, 1987; PDB file 1SRN), thus providing information relevant to the question of whether the crystallization solvent or interactions between molecules in the crystal lattice distort the structure of a protein significantly (Makinen & Fink, 1977; Zhang, Chance, Auld, Larsen & Vallee, 1992, and references therein).

## Materials and methods

*Preparation of RNase* 1–118 *and RNase* 111–124

RNase 1–118 was prepared from RNase A (type XII-A, Sigma) and characterized as previously described (de Mel *et al.*, 1992; de Mel, Doscher, Glinn *et al.*, 1994). The final purification step involves isocratic ion-exchange chromatography using a phosphate buffer. RNase 111–124 was synthesized by the Wayne State University Macromolecular Core Facility, and purified and characterized as previously described (Doscher *et al.*, 1983).

*Crystallization*

A salt-free aqueous solution of RNase 1–118 (11.9 mg) and RNase 111–124 (2.8 mg) (mole ratio 1:2) was freeze-dried, the residue was dissolved in 250 µl $H_2O$ in a small screw-capped vial and the pH adjusted to 5.3. A 188 µl aliquot of ethanol was added to provide 43%(*v*/*v*) aqueous ethanol and the solution was seeded with microcrystals of RNase A. Diffraction-quality crystals, 0.4 × 0.2 × 0.2 mm in size, appeared after a few months at room temperature.

*Data collection*

Area-detector data were collected at room temperature on a Siemens system employing a four-circle goniometer with a Rigaku RU200H rotating-anode generator operated at 40 kV and 70 mA, a Supper graphite monochromator, a 0.3 mm collimator, and the *Xengen* software package (Howard *et al.*, 1987) supported on a Silicon Graphics Personal IRIS minicomputer. The crystal was mounted in a quartz capillary in a random orientation, the detector was moved 12.0 cm away from the crystal and $2\theta$ was set at 25°. At 3 min a frame, a 0.25° oscillation in $\omega$ accumulated between two and three million counts. The data collection was organized using the program *ASTRO* (Chambers, Ortega & Campana, 1992) and additional data were collected by moving $2\theta$ to 40°. These data were indexed, merged, and scaled ($R_{sym}$ = 3.3), yielding 12 742 reflections, which represent 72% of the possible reflections to 1.6 Å resolution. In the shell extending from 1.67 to 1.60 Å, 54% of the data was observed. Intensities were reduced to structure amplitudes with the *Xengen* program using three alternating runs of *P*1 scaling (15–20 cycles) and batch deletions with $Q$ values of 9, 6, and a final $Q$ value determined by the software, followed by one last scaling run.

*Refinement*

The crystals belong to the same space group as RNase A; therefore, RNase A coordinates (PDB file 5RSA; Wlodawer *et al.*, 1982; Wlodawer & Sjölin, 1983) were used as the initial model. A total of 120 cycles of rigid-body refinement reduced the $R$ factor to 0.250 for data from 7.0 to 2.0 Å. Then refinement by simulated annealing was performed with the *X-PLOR* program (Brünger, 1988) and data from 7.0 to 1.8 Å. All simulated-annealing refinements used the slow-cool annealing protocol with the dynamics temperature starting out at 4000 K and decreasing in intervals of 25 K to a final temperature of 0 K, with 25 steps (0.5 fs step$^{-1}$) of

Verlet dynamics at each temperature. Further refinement was carried out using the program *PROFFT* (Agarwal, 1978; Finzel, 1987) while checking the stereochemistry graphically using the program *TOM/FRODO* (Jones, 1985; Cambillau & Horjales, 1987).

Water molecules were added and retained if the electron-density peak: (1) appeared in $F_o - F_c$ maps at greater than $3.5\sigma$; (2) appeared in $2F_o - F_c$ maps at greater than $0.7\sigma$ and (3) the position was within hydrogen-bonding distance of an appropriate atom.

A total of 111 cycles of *PROFFT*, including 98 water molecules, dropped the *R* value to 0.180 for data from 7.0 to 1.6 Å, with root-mean-square (r.m.s.) deviations for bonds and $\omega$ angles of 0.020 and 1.7°, respectively. Finally, the *X-PLOR* program was used to refine only the *B* values in each monomer. 20 cycles of *B*-value refinement dropped the *R* factor to 0.166 for $2\sigma$ data from 7.0 to 1.6 Å. The program *PROCHECK* (Laskowski, MacArthur, Moss & Thornton, 1993) was used to evaluate the stereochemistry of the structure. A total of 91.2% of the residues were in the most favored regions (*A*, *B*, *L*) and the other 8.8% were in the additional allowed regions (*a*, *b*, *l*, *p*) of the Ramachandran plot. The PDB file number (Bernstein *et al.*, 1977) for the structure is 1SSC.*

Crystal packing diagrams were obtained with the program *TURBO-FRODO* (Bio-Graphics, c/o LCCMB, Faculté Médecine Nord, 13916 Marseille CEDEX 20, France). Intermolecular crystal packing contacts were determined using the program *CRISPACK*, which generates all symmetry-related and translated molecules. Interactions were considered only between pairs of atoms that are less than 4 Å apart, but are not covalently bound to one another. The *CRISPACK* program is available from Dr Rodier.

## Results

*Data collection, structure determination and refinement*

The diffraction data and final refinement statistics for the structural determination of RNase 1–118:111–124[EtOH] are summarized in Table 1. Crystals of RNase 1–118:111–124[EtOH] grown at pH 5.3 belong to the same space group, $P2_1$, as crystals of RNase A grown from aqueous 2-methyl-2-propanol at the same pH value (Wlodawer & Sjölin, 1983) and are isomorphous with them. This allowed PDB file 5RSA (Bernstein *et al.*, 1977) to be used as the initial model. The application of refinement procedures as described under *Materials and methods* led to a final model with an *R* factor of 0.166 for $2\sigma$ data from 7.0 to 1.6 Å (PDB file 1SSC). The program *PROCHECK* (Laskowski *et al.*, 1993) was used to evaluate the stereochemistry of the structure. A total of 91.2% of the residues was in the most favored regions (*A*, *B*, *L*) and the other 8.8% was in the additional allowed regions (*a*, *b*, *l*, *p*) of the Ramachandran plot.

Table 1. *Data collection and refinement*

Comparable values are also given for RNase A from aqueous 2-methyl-2-propanol and RNase 1–118:111–124[salt].

| Statistics | RNase 1–118:111–124[EtOH]* | RNase A† | RNase 1–118:111–124[salt]‡ |
|---|---|---|---|
| Space group | $P2_1$ | $P2_1$ | $P3_221$ |
| Unit cell (Å, °)§ | $a = 30.36$ | $a = 30.18$ | $a = b = 67.68$ |
| | $b = 38.34$ | $b = 38.40$ | $c = 65.01$ |
| | $c = 53.55$ | $c = 53.32$ | $\gamma = 120$ |
| | $\beta = 106.35$ | $\beta = 105.85$ | |
| Reflections used | 12742 | 7708 (X-ray); 4132 (neutron) | 12117 |
| Percent of total data (%) | 72 | 95.6 (X-ray) | 73 |
| Resolution (Å) | 7.0–1.6 | 10.0–2.0 | 10.0–1.8 |
| Final *R* factor | 0.166 | 0.159 (X-ray) | 0.204 |
| R.m.s. bonds (Å) | 0.020 | 0.023 | 0.025 |
| R.m.s. $\omega$ angle (°) | 1.7 | 3.4 | 1.6 |

* Crystallized from 43% aqueous ethanol, pH 5.3; Protein Data Bank file 1SSC.

† Crystallized from 43% aqueous 2-methyl-2-propanol, pH 5.3. Wlodawer & Sjölin (1983); Protein Data Bank file 5RSA.

‡ Crystallized from 1.3 *M* ammonium sulfate, 3.0 *M* cesium chloride, pH 5.2; Martin, Doscher & Edwards (1987); Protein Data Bank file 1SRN.

§ One molecule per asymmetric unit in every case.

## Comparison of RNase 1–118:111–124[EtOH] with RNase A from aqueous 2-methyl-2-propanol

*Main-chain atoms*

The r.m.s. deviation of the positions of the $C_\alpha$ atoms of residues 2–110 of RNase 1–118:111–124[EtOH] with respect to the corresponding $C_\alpha$ atoms of RNase A (PDB file 5RSA) is 0.15 Å, as calculated using the program *ALIGN* (Satow, Cohen, Padlan & Davies, 1986), indicating that the overall structure of the two molecules is virtually identical. As with crystals of RNase 1–118:111–124[salt] (Martin *et al.*, 1987; de Mel *et al.*, 1992; de Mel, Doscher, Glinn *et al.*, 1994), only a portion of each of the two chains of the semisynthetic enzyme is seen. There is good electron density for residues 1–112 of RNase 1–118 and for residues 114–124 of RNase 111–124, but no appreciable electron density for either copy of Asn113 or the extra copy of any of the other redundant residues.

The main-chain hydrogen-bonding patterns of RNase 1–118:111–124[EtOH] and RNase A are coincident (Fig. 2). A notable aspect of these patterns is the identity of the intermolecular backbone hydrogen bonding between RNase 1–118 and RNase 111–124 with the intramolec-

* Atomic coordinates and structure factors have been deposited with the Protein Data Bank, Brookhaven National Laboratory (Reference: 1SSC). Free copies may be obtained through The Managing Editor, International Union of Crystallography, 5 Abbey Square, Chester CH1 2HU, England (Reference: SE0172).

ular backbone hydrogen bonding in the corresponding portion of RNase A.

*General features of the solvent structure*

Applying the criteria described under *Materials and methods*, 98 crystallographically bound water molecules are found in RNase 1–118:111–124[EtOH]. Of this total, 48 are coincident with the 128 water molecules found in RNase A, that is, they are within 1.0 Å of a water molecule in that structure.* When the positions of the 115 crystallographically bound water molecules in crystals of RNase 1–118:111–124[salt] are compared with those in RNase A, only 29 are found to be common (de Mel *et al.*, 1992).

* In de Mel, Doscher, Glinn *et al.* (1994), it was erroneously stated that water molecules were considered common if they were within 0.30 Å. The distance criterion was actually 1.0 Å in this study as well.

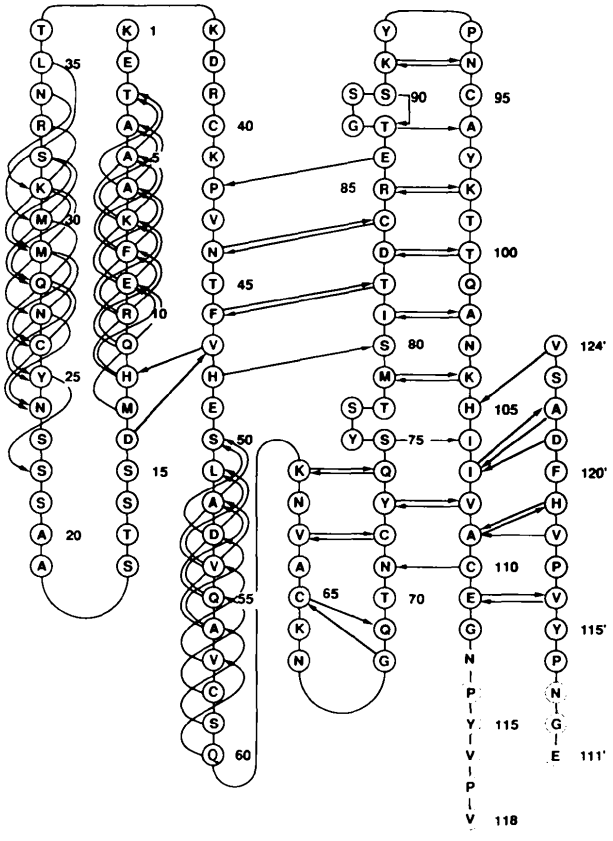

Fig. 2. Backbone hydrogen-bonding scheme for RNase 1–118:111–124 from aqueous ethanol. Backbone hydrogen bonds with a donor–acceptor distance less than 3.5 Å and an angle greater than 110° are shown for RNase 1–118:111–124 crystallized from aqueous ethanol. The arrows go from donor to acceptor. There is no appreciable electron density for residues 113–118 of RNase 1–118 or residues 111–113 of RNase 111–124. In RNase A, there is a peptide bond connecting Asn113 and Pro114; the backbone hydrogen bonding in this molecule is the same as that for the semisynthetic enzyme, however.

*Active-site residues*

Among the residues considered to be part of the active site of RNase are Gln11, His12, Lys41 and His119 (Richards & Wyckoff, 1971; Blackburn & Moore, 1982) (Fig. 3).

*Histidine* 12. The positioning of His12 is identical in the two structures with good hydrogen bonds seen from ND1 of the imidazole ring to the carbonyl O atom of Thr45 and from ND1 to the OD1 of Asn44 (Table 2).

*Histidine* 119. In contrast to our finding with RNase 1–118:111–124[salt] (Martin *et al.*, 1987), the side-chain positioning of this residue in the structure from aqueous ethanol corresponds very closely to that seen in RNase A by Wlodawer & Sjölin (1983) (Fig. 4). In this conformation, denoted position A, the NE2 N atom of the ring forms a good hydrogen bond with one of the O atoms of the $\beta$-carboxyl group of Asp121 (2.71 Å) and the ND1 N atom is hydrogen bonded to O1 of the phosphate (2.46 Å) (Table 2).

*Glutamine* 11. This residue, which has a hydrogen-bonding interaction with one of the O atoms of the phosphate anion bound at the active site (NE2 to O3 of the phosphate = 2.81 Å) (Table 2) and is invariant across


Fig. 3. Stereoview of RNase 1–118:111–124[EtOH]. Side chains of active-site residues Gln11, His12, Lys41 and His119 (in position *A*) are shown, as is phosphate anion 125, which is bound at the active site. The figure was obtained with the program *QUANTA*.

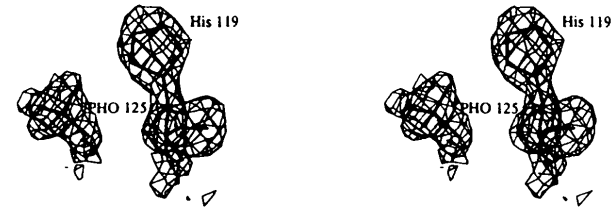


Fig. 4. Electron density for His119 in RNase 1–118:111–124 from aqueous ethanol. The $2F_o - F_c$ density peaks for the imidazole ring of His119 and for the phosphate ion in RNase 1–118:111–124 crystallized from aqueous ethanol contoured at 1.5$\sigma$. The side chain is in position *A*.

Table 2. *Selected hydrogen-bond distances* (Å) *at the active site of RNase* 1–118:111–124[*Et*OH], *RNase A from aqueous 2-methyl-2-propanol and RNase* 1–118:111–124[*salt*]

| Hydrogen bond | RNase 1–118: 111–124* | RNase A† | RNase 1–118: 111–124‡ |
|---|---|---|---|
| His12 ND1···Asn44 OD1 | 3.47 | 3.40 | 3.22 |
| His12 ND1···Thr45 O | 2.75 | 2.70 | 2.68 |
| His12 NE2···Sul125 O4 | — | — | 2.42 |
| His12 NE2···PHO125 O2 | 2.52 | 2.61 | — |
| His12 NE2···PHO125 O4 | 3.50 | 3.14 | — |
| His119 ND1···Sul125 O2 | — | — | 2.93 |
| His119 ND1···PHO125 O1 | 2.46 | 2.36 | — |
| His119 NE2···Asp121 OD1 | 2.71 | 2.74 | — |
| Lys41 NZ···Gln11 OE1 | 3.12 | — | 3.34 |
| Lys41 NZ···Asn44 OD1 | 2.83 | 2.90 | 2.93 |
| Lys41 NZ···PHO125 O4 | 2.90 | 3.04 | — |
| Lys41 N···Leu35 O | — | — | 3.11 |
| Gln11 O···Lys44 ND2 | 2.78 | 2.76 | 2.75 |
| Gln11 NE2···Sul125 O3 | — | — | 2.81 |
| Gln11 NE2···PHO125 O3 | 2.81 | — | — |
| Phe120 N···Sul125 O4 | — | — | 3.25 |
| Phe120 N···PHO125 O2 | 3.06 | 2.84 | — |
| Lys66 N···Asp121 OD2 | 3.02 | 2.90 | 3.17 |
| Lys66 NZ···Asp121 OD1 | 2.76 | 2.84 | 3.44 |

* Crystallized from 43% aqueous ethanol, pH 5.3; Protein Data Bank file 1SSC.

† Crystallized from 43% aqueous 2-methyl-2-propanol, pH 5.3. Wlodawer & Sjölin (1983); Protein Data Bank file 5RSA.

‡ Crystallized from 1.3 *M* ammonium sulfate, 3.0 *M* cesium chloride, pH 5.2; Martin, Doscher & Edwards (1987); Protein Data Bank file 1SRN.

Table 3. *Crystal packing interactions of RNase* 1–118:111–124[*Et*OH]

RNase 1–118:111–124[EtOH] was crystallized from 43% aqueous ethanol, pH 5.3; Protein Data Bank file 1SSC.

| Transformations | Interactions: van der Waals | Hydrogen bonds | Salt bridges | No. of residues involved |
|---|---|---|---|---|
| $-1+x \quad y \quad z$ | 6 | 1 | — | 4 |
| $x \quad -1+y \quad z$ | 14 | 1 | — | 4 |
| $x \quad 1+y \quad z$ | 14 | 1 | — | 5 |
| $1+x \quad y \quad z$ | 6 | 1 | — | 4 |
| $1-x \quad -\frac{1}{2}+y \quad -z$ | 4 | 2 | — | 3 |
| $1-x \quad \frac{1}{2}+y \quad -z$ | 4 | 2 | — | 1 |
| $2-x \quad -\frac{1}{2}+y \quad -z$ | 34 | 1 | 2 | 3 |
| $2-x \quad -\frac{1}{2}+y \quad 1-z$ | 23 | 5 | — | 4 |
| $2-x \quad \frac{1}{2}+y \quad -z$ | 34 | 1 | 2 | 5 |
| $2-x \quad \frac{1}{2}+y \quad 1-z$ | 23 | 5 | — | 5 |
| Totals | 162 | 20 | 4 | 38* |

* 35 residues contact 35 residues. Residues 1, 70, and 92 are each involved in two contacts, however.

40 species of mammalian pancreatic RNases (Beintema, Schuller, Irie & Carsana, 1988), occupies an exactly coincident position in the semisynthetic enzyme and in RNase A.

*Lysine* 41. Good electron density is seen for all the side-chain atoms of this residue, which is also invariant (Beintema *et al.*, 1988) and is thought to participate during catalysis in the stabilization of the transition state (Hirs, Halmann & Kycia, 1965; Deavin, Mathias & Rabin, 1966; Roberts, Dennis, Meadows, Cohen & Jardetzky, 1969; Lim & Tole, 1992, and references therein). The NZ atom has moved 0.28 Å away from the active site with respect to its position in RNase A, but its hydrogen-bonding pattern remains unchanged (Table 2).

*Active-site solvent molecules*

The water molecule ubiquitously found in all previous refined structures where a sulfate or phosphate is present at the active site (Wlodawer & Sjölin, 1983; Borkakoti, Moss, Stanford & Palmer, 1984; Martin *et al.*, 1987; Kim, Varadarajan, Wyckoff & Richards, 1992; de Mel *et al.*, 1992; de Mel, Doscher, Glinn *et al.*, 1994) is also seen in RNase 1–118:111–124[EtOH]. It is stabilized by three good hydrogen bonds: to NE2 of Gln11 (2.63 Å), to O2 of the phosphate (2.77 Å), and to O3 of the phosphate (3.01 Å) (Table 2). The *B* value for this water molecule (WAT141) is 17.4 Å$^2$, which is very similar to the value of 18 Å$^2$ found for the semisynthetic enzyme from salt solutions (de Mel *et al.*, 1992), but significantly higher than the *B* value of 9.9 Å$^2$ seen in RNase A (Wlodawer & Sjölin, 1983).

*Active-site anion*

Based on the preparative history of RNase 1–118 and the conditions used for crystallization (see *Materials and methods*), we are assuming phosphate to be the anionic ligand at the active site of RNase 1–118:111–124[EtOH]. The position, the orientation, and the hydrogen-bonding partners of the O atoms of this phosphate are all the same as those found for the phosphate ligand in RNase A (Wlodawer & Sjölin, 1983) (Table 2).

*Multiple conformations*

Two conformations are observed for nine residues in RNase 1–118:111–124[EtOH]: Lys1, Lys7, Val43, Lys66, Ser77, Asp83, Arg85, Asp103 and Lys104. In RNase A from aqueous 2-methyl-2-propanol, 13 residues were found to have two conformations (Svensson, Sjölin, Gilliland, Finzel & Wlodawer, 1986). However, only five of these residues, namely, Val43, Ser77, Asp83, Arg85 and Lys104, are common to both structures. The triplet of Val43, Asp83 and Arg85, which Svensson *et al.* (1986) conclude must undergo a concerted conformation change, has also been found to have two conformations in RNase S crystallized from salt solutions (Kim *et al.*, 1992).

*Intermolecular contacts*

In crystals of phosphate-free RNase A grown from aqueous 2-methyl-2-propanol (space group $P2_1$) (Wlodawer, Svensson, Sjölin & Gilliland, 1988; PDB file 7RSA), each molecule is found to interact with ten symmetry-related neighbors (Svensson *et al.*, 1991;

Crosio, Janin & Jullien, 1992). These intermolecular contacts involve a total of 35 surface residues and include hydrogen bonds, salt bridges, and numerous van der Waals interactions. A packing diagram for space group $P2_1$ is given in Fig. 5. With one exception, the same set of interactions is seen for each molecule of RNase 1–118:111–124[EtOH] (Table 3). The exception involves the replacement of the Glu9:Lys61/Lys61:Glu9 interactions seen in RNase A with Thr3:Lys91/Lys91:Thr3 interactions in RNase 1–118:111–124[EtOH]. This difference may reflect the fact that Lys61 and Lys91 have dual conformations in RNase A, but not in RNase 1–118:111–124[EtOH].

## Comparison of the structures of RNase 1–118:111–124[EtOH] and RNase 1–118:111–124[salt]

### *Main-chain atoms*

The r.m.s. deviation of the positions of the $C_\alpha$ atoms of residues 2–110 of RNase 1–118:111–124[EtOH] with respect to the corresponding $C_\alpha$ atoms of the semisynthetic enzyme from salt solutions (Martin *et al.*, 1987; PDB file 1SRN) is 0.39 Å, indicating that the overall structure of the two molecules is very similar, but not quite so coincident as the structure of the semisynthetic enzyme from aqueous ethanol and RNase A from aqueous 2-methyl-2-propanol. However, with one exception (see under *Lysine* 41, below), all main-chain hydrogen-bonding interactions are the same in the two structures.

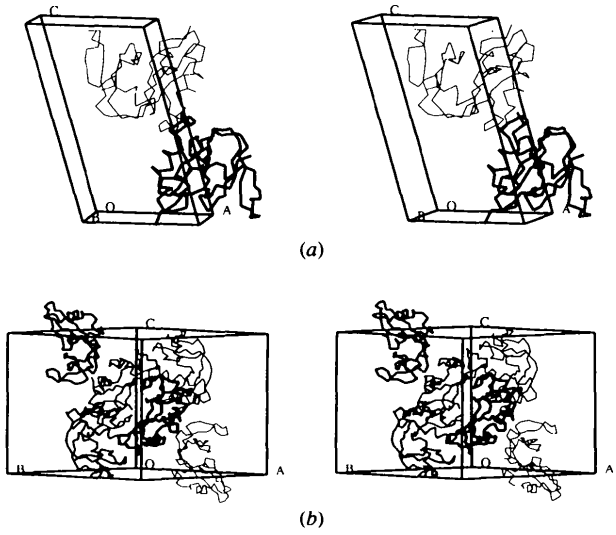


Fig. 5. Crystal packing of RNase 1–118:111–124[EtOH] and RNase 1–118:111–124[salt]. (*a*) Stereoview of the cell contents of RNase 1–118:111–124[EtOH]. There are only two molecules in the unit cell and they are related to one another by a twofold screw axis parallel to *b*. (*b*) Stereoview of the cell contents of RNase 1–118:111–124[salt]. The threefold screw axis is parallel to *c*. The view is along the axis of twofold symmetry relating the two monomers in the 'dimer'. The plots were obtained with the program *TURBO-FRODO*.

There are, however, differences in backbone structure in the loop regions represented by residues 35–43, 65–72 and 85–94, with a maximal deviation of 1.59 Å seen at residue 89 (Fig. 6).

### *General features of the solvent structure*

When the positions of the 115 crystallographically bound water molecules in crystals of RNase 1–118:111–124[salt] are compared with the 98 water molecules in RNase 1–118:111–124[EtOH], only 21 are found to coincide. With the semisynthetic enzyme from aqueous ethanol and RNase A from aqueous 2-methyl-2-propanol, 48 overlapping waters were seen (see above).

### *Active-site residues*

The positions of His12 and Glu11 correspond very closely in RNase 1–118:111–124[EtOH] and RNase 1–118:111–124[salt], with all the hydrogen-bonding interactions seen for these residues being the same (Table 2).

*Histidine* 119. The major difference between the structure of RNase 1–118:111–124 from aqueous ethanol and from salt solutions is the location of the imidazole ring of His119. In the structure from salt solutions, the side chain has a conformation, denoted position *B*, where the $\chi_1$ value is –47° (Martin *et al.*, 1987), but in the structure from aqueous ethanol, it takes up an alternative conformation, denoted position *A*, which has a $\chi_1$ value of +162°. Transition between these two conformations can occur by rotation about the $C_\alpha$—$C_\beta$ bond. In their early structural analysis of RNase S, Wyckoff & Richards and coworkers concluded that His119 assumed multiple conformations (Wyckoff *et al.*, 1970). A description of the dual positioning was first given by Borkakoti, Moss & Palmer (1982) and

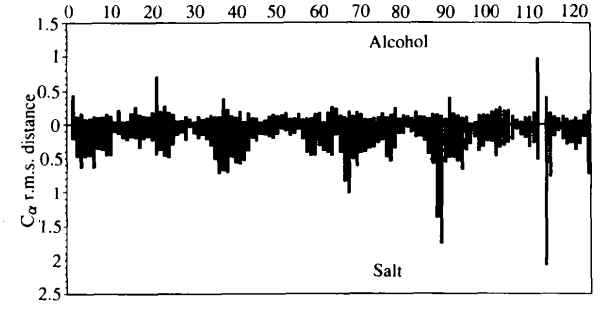


Fig. 6. R.m.s. displacements of RNase 1–118:111–124 from aqueous ethanol compared with RNase A and with RNase 1–118:111–124 from salt solutions. R.m.s. displacements of main-chain and side-chain atoms: (top) aqueous ethanol structure relative to RNase A, and (bottom) aqueous ethanol structure relative to salt solution structure, plotted as a function of residue number.

Borkakoti *et al.* (1984), who reported a minor occupancy (20%) for His119 in RNase A crystallized from aqueous ethanol at pH 5.2–5.7, which they denoted as position *B*. The major occupancy (80%) was denoted position *A*. In the structures of RNase A determined by Wlodawer and coworkers, His119 was found to be exclusively in position *A* (Wlodawer *et al.*, 1982; Wlodawer & Sjölin, 1983). On the other hand, position *B* is the predominant or sole conformation seen for His119 in crystals of RNase 1–118:111–124[salt] and several analogs thereof at pH 5.2 (Martin *et al.*, 1987; de Mel *et al.*, 1992; de Mel, Doscher, Glinn *et al.*, 1994), in crystals of a His12 alkylated derivative of RNase A (Nachman *et al.*, 1990), in crystals of a refined structure of RNase S (Kim *et al.*, 1992) and in crystals of bovine seminal RNase (Mazzarella *et al.*, 1993).

As the pH of crystals of RNase 1–118:111–124[salt] is raised from pH 5.2 to 8.8, a progressive conversion of the side chain of His119 to position *A* is observed (de Mel, Doscher, Martin *et al.*, 1994). Recently, a high-resolution NMR study of RNase A has revealed that position *B* also predominates in solution at pH 4.0, with conversion to position *A* occurring as the pH is raised (Rico *et al.*, 1991; Santoro *et al.*, 1993).

*Lysine* 41. In the structure of RNase 1–118:111–124[EtOH], the NZ of Lys41 forms a good hydrogen bond with one of the O atoms of the active-site phosphate (NZ···PHO125 O4 = 2.90 Å). No corresponding bond is found between NZ and one of the O atoms of the active-site sulfate in RNase 1–118:111–124[salt]. There is a hydrogen bond between Lys41 and Leu35 that is found only in the structure from salt solutions, however (Table 2).

*Lysine* 66. In the structure of RNase A and the structure of RNase 1–118:111–124[EtOH], the two hydrogen-bonding interactions between the $\beta$-carboxyl group of Asp121 and Lys66 are identical with respect both to the atoms involved and the lengths of the bonds formed (Table 2). In the structure of RNase 1–118:111–124[salt], the interaction between the backbone N atom of Lys66 and OD2 of Asp121 is also the same, but the hydrogen bond between NZ of Lys66 and OD1 of Asp121 is significantly lengthened (Table 2).

*Active-site solvent molecules*

As noted above, the water molecule found in structures containing a sulfate or a phosphate at the active site is present in RNase 1–118:111–124 from both aqueous ethanol and concentrated salt solutions. It occupies a coincident position in the two structures and has *B* values of 17.4 and 18 Å$^2$, respectively.

*Active-site anion*

In RNase 1–118:111–124[salt], sulfate is the anion at the active site rather than the phosphate assumed to be present in the structure from aqueous ethanol. The general positioning of the two anions is very similar, although the sulfate is shifted 0.4 Å and rotated approximately 30° with respect to the phosphate. As a consequence, the hydrogen-bonding interactions of the two anions differ (Table 2). Most noteworthy is the switch from a His12 NE2···O hydrogen bond in high salt solutions to a Lys41 NZ···O hydrogen bond in aqueous ethanol.

*Intermolecular interactions*

A comparative analysis of the intermolecular contacts in RNase 1–118:111–124 crystals grown from salt (space group $P3_221$) and from aqueous ethanol (space group $P2_1$) reveals a divergence in the nature of the contacts to the extent where they are almost, but not quite, mutually exclusive (Fig. 7). Packing diagrams for space groups $P3_221$ and $P2_1$ are given in Fig. 5. A comparable degree of difference in intermolecular interactions has been seen in crystals of a modified RNase A grown from salt solutions and crystals of RNase A grown from aqueous alcohol solutions (Svensson *et al.*, 1991; Crosio *et al.*, 1992). With salt solutions, a dominating set of interactions occurs at one interface, leading to the appearance of a dimer-like structure under these conditions, and, indeed, a dimeric intermediate has been found on the salt-induced crystallization pathway of RNase A (Jullien, Crosio, Baudet-Nessler, Mérola & Brochon, 1994). In addition, the various interfaces seen in salt-grown crystals are enriched in non-polar and charged groups and depleted in neutral polar groups relative to the interfaces seen in alcohol-grown crystals (Crosio *et al.*, 1992).

## Discussion

On the basis of the relative magnitude of overlap of the $C_\alpha$ atoms in residues 2–110 (r.m.s. deviation = 0.15 Å), the structure of RNase 1–118:111–124[EtOH] resembles that of RNase A from aqueous 2-methyl-

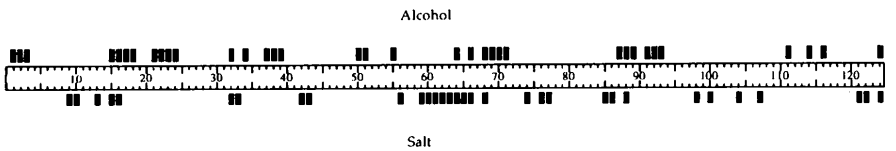


Fig. 7. Intermolecular contacts in crystals of RNase 1–118:111–124 grown from aqueous ethanol and from concentrated salt solutions. Numbers refer to residue number. Contacts were identified using the program *CRISPACK* (see *Materials and methods*).

2-propanol more closely than it does the structure of RNase 1–118:111–124[salt] (r.m.s. deviation = 0.39 Å), although all three structures are very similar in most respects.

Given the great similarity between the structures of RNase 1–118:111–124[EtOH] and RNase A from aqueous 2-methyl-2-propanol, the coincidence of less than 50% in the positions of the water molecules in the two structures is instructive. It seems unlikely that the replacement of 2-methyl-2-propanol by ethanol is a factor. King, Magdoff, Adelman & Harker (1956) found that the unit-cell dimensions of RNase A crystals (space group $P2_1$) varied no more than 0.2 Å (< 0.7%) whether the mother liquor was an aqueous mixture with methanol, ethanol, 2-methyl-2-propanol or 2-methyl-2,4-pentanediol.

Additionally, Tilton, Dewan & Petsko (1992) determined that changing the mother liquor from 2-methyl-2,4-pentanediol to methanol between 220 and 240 K had no apparent effect on the structure of RNase A. It is true, of course, that eight redundant residues are present in the semisynthetic enzyme even though no electron density is seen for them. Nonetheless, it seems unlikely that this difference alone would disturb the positioning of 50 water molecules. A fairly good correlation does exist, however, between the temperature factors of the water molecules and their positional coincidence in the two structures (Fig. 8). If we take the view that the positional coincidence of the water molecules in these two proteins is a measure of their reality, we see that the probability of encountering artifactual water molecules becomes very high when temperature factors rise above 40 Å$^2$. In their rigorous study of solvent structure in erabutoxin b, Smith, Corfield, Hendrickson & Low (1988) found only two of the 111 water sites in the final model to have a $B$ value of 40 Å$^2$ or above.

It is evident by now that His119 exhibits a conformational mobility that is unique among the amino-acid residues comprising the active site of RNase. By

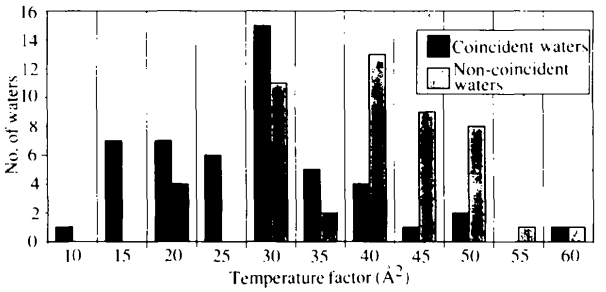


Fig. 8. Coincident water molecules *versus* temperature factors. The number of coincident and non-coincident water molecules in RNase A from aqueous 2-methyl-2-propanol and RNase 1–118:111–124 from aqueous ethanol as a function of temperature factor. The black bars represent coincident water molecules and the shaded bars represent non-coincident water molecules. Two water molecules are considered coincident if they are located within 1.0 Å of one another.

rotation about its $C_\alpha$—$C_\beta$ bond, the imidazole side chain can occupy two distinct conformations, denoted position $A$ ($\chi_1$ = +149 to +162°) and position $B$ ($\chi_1$ = −47 to −76°). The relative occupancy of the two conformations in the crystal appears to be modulated by the crystallization solvent, with position A being favored in aqueous organic solvents (Borkakoti *et al.*, 1982; Wlodawer & Sjölin, 1983; and as reported herein) and position $B$ being favored in salt solutions (Martin *et al.*, 1987; Nachman *et al.*, 1990; Kim *et al.*, 1992). The equilibrium between the two conformations also seems to be a function of pH, both in solution (Rico *et al.*, 1989; Santoro *et al.*, 1993) and in the crystal (de Mel, Doscher, Martin *et al.*, 1994), with position $B$ being favored at low pH values and position $A$ being favored at high pH values. Harris, Borkakoti, Moss, Palmer & Howlin (1987) have reported that a non-bonded potential energy map for His119 reveals two discrete side-chain positions possessing energy minima. These positions correspond to the crystallographically observed $A$ and $B$ positions and are linked by a low-energy pathway.

The observed mobility of His119 may reflect local changes in dielectric constant induced by a change in pH or crystallization solvent. RNase is a basic protein with an isoionic point of 9.6 (Richards & Wyckoff, 1971). Consequently, at pH 5.2, where crystals of RNase 1–118:111–124 are grown, the net positive charge on the molecule is approximately 8. Also, if we assume the p$K$ value for the side chain of His119 to be comparable at high and low salt concentrations, His119 will be positively charged in roughly 90% of the molecules at pH 5.2. Under these conditions, position $B$ is presumably the conformation with the lower energy when the protein is in a concentrated salt solution. If the dielectric constant in the region of position $B$ is greatly reduced by moving to an aqueous ethanol solution, however, then position $A$ may become the conformation with a relatively lower energy. In the same way, raising the pH, which both reduces the net positive charge on the protein and abolishes the positive charge on His119, could reduce the relative energy cost of occupying position $A$.

Given the central role ascribed to His119 in the catalytic mechanism of RNase (Brooks *et al.*, 1986; Lim & Tole, 1992), the possibility that the dual positioning has mechanistic significance is an attractive idea. In their studies of the active-site dynamics of RNase A, Brünger, Brooks & Karplus (1985) noted that His119 underwent dihedral-angle transitions in some of the simulations and suggested that this freedom of movement might be important for the catalytic mechanism. Modeling studies by de Mel *et al.* (1992) have revealed, however, that His119 can participate in both the transphosphorylation and hydrolytic reactions catalyzed by RNase whether in position $A$ or position $B$.

As yet, no further experimental indication or disproof of a linkage between the dual conformations of His119

and the mechanism of action of the enzyme has been forthcoming.

As was the case concerning crystallographically bound water molecules, a comparison of the residues found to be in multiple conformations in RNase 1–118:111–124[EtOH] and RNase A from aqueous 2-methyl-2-propanol has revealed a surprisingly high disparity in the assignments: only five of the total of 17 such residues are common to both structures. Of these five residues, three (Val43, Asp83 and Arg85) appear to undergo a concerted conformational change (Svensson *et al.*, 1986). Multiple conformations have also been seen for each of these residues in RNase S crystallized from salt solutions (Kim *et al.*, 1992). The three residues line the active-site cleft; nevertheless, none is found to be invariant among mammalian pancreatic RNases (Beintema *et al.*, 1988).

In contrast to the variation in the location of crystallographically bound water or in those residues found in multiple conformations, there is almost complete coincidence in the nature of the intermolecular contacts seen in RNase 1–118:111–124[EtOH] and in RNase A from aqueous 2-methyl-2-propanol. The intermolecular contacts seen in the semisynthetic enzyme from salt solutions are almost completely different, however, indicating that crystallization solvent plays a major role in determining the nature of these contacts, an observation in agreement with the findings of Crosio *et al.* (1992).

Thus, we conclude that the nature of the crystallization solvent or of the intermolecular contacts in the crystal lattice does not affect the large-scale structural elements of the protein significantly. Nonetheless, the crystallization solvent does determine which set of the residues will make intermolecular contacts with the result that the residues making these contacts can vary greatly. An additional effect that is particularly noteworthy is the modulation of the conformation of an active-site residue by the crystallization solvent. Whether determined by solvent effects, intermolecular contacts or other factors, many differences in the positioning of crystallographically bound water are also seen, as are differences in the selection of residues found to have multiple conformations.

This work was supported in part by NIH Grant GM 40630. Amino-acid and Edman sequence analyses as well as peptide syntheses were performed by the Wayne State University Macromolecular Core Facility.

## References


AGARWAL, R. C. (1978). *Acta Cryst.* A**34**, 791–809.

BEINTEMA, J. J., SCHULLER, C., IRIE, M. & CARSANA, A. (1988). *Prog. Biophys. Mol. Biol.* **51**, 165–192.

BERNSTEIN, F. C., KOETZLE, T. F., WILLIAMS, G. J. B., MEYER, E. F., BRICE, M. D., RODGERS, G. R., KENNARD, O., SHIMANOUCHI, T. & TASUMI, M. (1977). *J. Mol. Biol.* **112**, 535–542.

BLACKBURN, P. & MOORE, S. (1982). *Pancreatic Ribonuclease.* In *The Enzymes*, 3rd Ed., Vol. 4, edited by P. D. BOYER, pp. 317–433. New York: Academic Press.

BORKAKOTI, N., MOSS, D. S. & PALMER, R. A. (1982). *Acta Cryst.* B**38**, 2210–2217.

BORKAKOTI, N., MOSS, D. S., STANFORD, M. J. & PALMER, R. A. (1984). *J. Crystallogr. Spectrosc. Res.* **14**, 467–494.

BROOKS, C. III, BRÜNGER, A., FRANCL, M., HAYDOCK, K., ALLEN, L. C. & KARPLUS, M. (1986). *Ann. NY Acad. Sci.* **471**, 295–298.

BRÜNGER, A. T. (1988). *J. Mol. Biol.* **203**, 803–816.

BRÜNGER, A. T., BROOKS, C. L. III & KARPLUS, M. (1985). *Proc. Natl Acad. Sci. USA*, **82**, 8458–8462.

CAMBILLAU, C. & HORJALES, E. (1987). *J. Mol. Graphics*, **5**, 174–177.

CEDERHOLM, M. T., STUCKEY, J. A., DOSCHER, M. S. & LEE, L. (1991). *Proc. Natl Acad. Sci. USA*, **88**, 8116–8120.

CHAMBERS, J. L., ORTEGA, R. B. & CAMPANA, C. F. (1992). Amer. Crystallogr. Assoc., 50th Annual Meet., Abstract PA 27.

CROSIO, M.-P., JANIN, J. & JULLIEN, M. (1992). *J. Mol. Biol.* **228**, 243–251.

DEAVIN, A., MATHIAS, A. P. & RABIN, B. R. (1966). *Nature (London)*, **211**, 252–255.

DOSCHER, M. S., MARTIN, P. D. & EDWARDS, B. F. P. (1983). *Biochemistry*, **22**, 4125–4131.

FINZEL, B. C. (1987). *J. Appl. Cryst.* **20**, 53–55.

GUTTE, B., LIN, M. C., CALDI, D. G. & MERRIFIELD, R. B. (1972). *J. Biol. Chem.* **247**, 4763–4767.

HARRIS, G. W., BORKAKOTI, N., MOSS, D. S., PALMER, R. A. & HOWLIN, B. (1987). *Biochim. Biophys. Acta*, **912**, 348–356.

HIRS, C. H. W., HALMANN, M. & KYCIA, J. H. (1965). *Arch. Biochem. Biophys.* **111**, 209–222.

HODGES, R. S. & MERRIFIELD, R. B. (1974). *Int. J. Pept. Protein Res.* **6**, 397–405.

HODGES, R. S. & MERRIFIELD, R. B. (1975). *J. Biol. Chem.* **250**, 1231–1241.

HOWARD, A. J., GILLILAND, G. L., FINZEL, B. C., POULOS, T. L., OHLENDORF, D. H. & SALEMME, F. R. (1987). *J. Appl. Cryst.* **20**, 383–387.

JONES, T. A. (1985). *Methods. Enzymol.* **115**, 157–171.

JULLIEN, M., CROSIO, M.-P., BAUDET-NESSLER, S., MÉROLA, F. & BROCHON, J.-C. (1994). *Acta Cryst.* D**50**, 398–403.

KIM, E. E., VARADARAJAN, R., WYCKOFF, H. W. & RICHARDS, F. M. (1992). *Biochemistry*, **31**, 12304–12314.

KING, M. V, MAGDOFF, B. S., ADELMAN, M. B. & HARKER, D. (1956). *Acta Cryst.* **9**, 460–465.

LASKOWSKI, R. A., MACARTHUR, M. W., MOSS, D. S. & THORNTON, J. M. (1993). *J. Appl. Cryst.* **26**, 283–291.

LIM, C. & TOLE, P. (1992). *J. Am. Chem. Soc.* **114**, 7245–7252.

LIN, M. C. (1970). *J. Biol. Chem.* **245**, 6726–6731.

LIN, M. C., GUTTE, B., CALDI, D. G., MOORE, S. & MERRIFIELD, R. B. (1972). *J. Biol. Chem.* **247**, 4768–4774.

LIN, M. C., GUTTE, B., MOORE, S. & MERRIFIELD, R. B. (1970). *J. Biol. Chem.* **245**, 5169–5170.

MAKINEN, M. W. & FINK, A. L. (1977). *Annu. Rev. Biophys. Bioeng.* **6**, 301–343.

MARTIN, P. D., DOSCHER, M. S. & EDWARDS, B. F. P. (1987). *J. Biol. Chem.* **262**, 15930–15938.

MAZZARELLA, L., CAPASSO, S., DEMASI, D., DI LORENZO, G., MATTIA, C. A. & ZAGARI, A. (1993). *Acta Cryst.* D**49**, 389–402.

DE MEL, V. S. J., MARTIN, P. D., DOSCHER, M. S. & EDWARDS, B. F. P. (1992). *J. Biol. Chem.* **267**, 247–256.

DE MEL, V. S. J., DOSCHER, M. S., GLINN, M. A., MARTIN, P. D., RAM, M. L. & EDWARDS, B. F. P. (1994). *Protein Sci.* **3**, 39–50.

DE MEL, V. S. J., DOSCHER, M. S., MARTIN, P. D. & EDWARDS, B. F. P. (1994). *FEBS Lett.* **349**, 155–160.

MERRIFIELD, R. B. & HODGES, R. S. (1975). *Synthetic approaches to the study of proteins.* In *Proceedings of the International Symposium on Macromolecules*, edited by E. B. MANO, pp. 417–431. Amsterdam: Elsevier

NACHMAN, J., MILLER, M., GILLILAND, G. L., CARTY, R., PINCUS, M. & WLODAWER, A. (1990). *Biochemistry*, **29**, 928–937.

RICHARDS, F. M. & WYCKOFF, H. W. (1971). *Bovine Pancreatic Ribonuclease*. In *The Enzymes*, Vol. 4, edited by P. D. BOYER, pp. 647–806. New York: Academic Press.

RICO, M., BRUIX, M., SANTORO, J., GONZALEZ, C., NEIRA, J. L., NIETO, J. L. & HERRANZ, J. (1989). *Eur. J. Biochem.* **183**, 623–638.

RICO, M., SANTORO, J., GONZALEZ, C., BRUIX, M., NEIRA, J. L., NIETO, J. L. & HERRANZ, J. (1991). *J. Biomol. NMR*, **1**, 283–298.

ROBERTS, G. C. K., DENNIS, E. A., MEADOWS, D. H., COHEN, J. S. & JARDETZKY, O. (1969). *Proc. Natl Acad. Sci. USA*, **62**, 1151–1158.

SANTORO, J., GONZALEZ, C., BRUIX, M., NEIRA, J. L., NIETO, J. L., HERRANZ, J. & RICO, M. (1993). *J. Mol. Biol.* **229**, 722–734.

SATOW, Y., COHEN, G. H., PADLAN, E. A. & DAVIES, D. R. (1986). *J. Mol. Biol.* **190**, 593–604.

SERDIJN, J., BLOEMHOFF, W., KERLING, K. E. T. & HAVINGA, E. (1984*a*). *Recl. Trav. Chim. Pays-Bas*, **103**, 50–54.

SERDIJN, J., BLOEMHOFF, W., KERLING, K. E. T. & HAVINGA, E. (1984*b*). *Recl. Trav. Chim. Pays-Bas*, **103**, 351–360.

SERDIJN, J., HOES, C., RAAP, J. & KERLING, K. E. T. (1980). *Recl. Trav. Chim. Pays-Bas*, **99**, 349–352.

SMITH, J. L., CORFIELD, P. W. R., HENDRICKSON, W. A. & LOW, B. W. (1988). *Acta Cryst.* A**44**, 357–368.

STERN, M. S. & DOSCHER, M. S. (1984). *FEBS Lett.* **171**, 253–255.

SVENSSON, L. A., DILL, J., SJÖLIN, L., WLODAWER, A., TONER, M., BACON, D., MOULT, J., VEERAPANDIAN, B. & GILLILAND, G. L. (1991). *J. Cryst. Growth*, **110**, 119–130.

SVENSSON, L. A., SJÖLIN, L., GILLILAND, G. L., FINZEL, B. C. & WLODAWER, A. (1986). *Proteins*, **1**, 370–375.

TILTON, R. F., DEWAN, J. C. & PETSKO, G. A. (1992). *Biochemistry*, **31**, 2469–2481.

WLODAWER, A., BOTT, R. & SJÖLIN, L. (1982). *J. Biol. Chem.* **257**, 1325–1332.

WLODAWER, A. & SJÖLIN, L. (1983). *Biochemistry*, **22**, 2720–2728.

WLODAWER, A., SVENSSON, L. A., SJÖLIN, L. & GILLILAND, G. L. (1988). *Biochemistry*, **27**, 2705–2717.

WYCKOFF, H. W., TSERNOGLOU, D., HANSON, A. W., KNOX, J. R., LEE, B. & RICHARDS, F. M. (1970). *J. Biol. Chem.* **245**, 305–328.

ZHANG, K., CHANCE, B., AULD, D. S., LARSEN, K. S. & VALLEE, B. L. (1992). *Biochemistry*, **31**, 1159–1168.